Slow gravity-driven migration and interaction of a bubble and a solid particle near a free surface

Marine Guémas, Antoine Sellier, Franck Pigeonneau

Slow gravity-driven migration and interaction of a bubble and a solid particle near a free surface

M. Guémas[1,2], A. Sellier[1] and F. Pigeonneau[2]
[1]LadHyx. Ecole polytechnique, 91128 Palaiseau Cédex, France
[2]Surface du Verre et Interfaces, UMR125 CNRS St Gobain, 39 quai Lucien Lefranc, BP 135, 93303 Aubervilliers, Cedex, France
marine.guemas@ladhyx.polytechnique.fr, sellier@ladhyx.polytechnique.fr, Franck.Pigeonneau@saint-gobain.com

Keywords: Free surface, bubble, solid particle, surface tension, axisymmetric Stokes flow, Boundary-integral equation.

Abstract. The axisymmetric gravity-driven migration of two interacting bubble and solid particle near a free surface is examined. The solid particle location and the bubble and free surface shapes are numerically tracked in time. This is done by solving at each time step a steady Stokes problem (with mixed-type boundary conditions) owing to a boundary approach which makes it possible to reduce the task to the treatment of two boundary-integral equations on the unbounded liquid domain boundary. The theoretical material and the relevant numerical implementation, valid for a bubble and a free surface with either equal or unequal uniform surface tensions, are briefly described and preliminary numerical results for a nearly-neutrally buoyant solid sphere interacting with a bubble and a free surface with equal surface tensions are presented.

Introduction

In basic applications (geophysics, glass process,...) it is important to determine the gravity-driven migration of clusters of non-rigid bubbles immersed in a liquid near a free surface. Such a task is involved since the bubbles and free surface shapes are unknown and time-dependent. Moreover, the liquid flow is in general governed by the unsteady Navier-Stokes equations. Fortunately, for small "enough" bubbles one can neglect inertial effects therefore arriving at a much more tractable creeping flow quasi-steady problem. Within this convenient framework, Pigeonneau & Sellier [1] recently proposed a boundary approach to efficiently deal with axisymmetric configurations obtained when the free surface and the bubbles share the same axis of symmetry aligned with the imposed uniform gravity $\mathbf{g}$. Later Guémas et al. [2] extended [1] to the case of bubbles and free surface not necessarily having the same surface tension. However, one also encounters in practice clusters made of both bubbles and solid particles. For instance, in liquid glass nearly neutrally buoyant solid impurities coexist with bubbles and it is important to investigate to which extent such solid particles affect the migration of the bubbles. To deal with this issue, still in axisymmetric configurations, Guémas et al. [3] proposed a theoretical boundary formulation for clusters made of $M \geq 1$ bubble(s) and $N \geq 1$ not-necessarily spherical solid particles consisting in (numerically) inverting $N+1$ relevant boundary-integral equations on the liquid domain boundary (i. e. the free surface and the cluster's boundary). This paper presents preliminary numerical results for a neutrally buoyant solid sphere interacting with one bubble and a free surface having identical surface tensions.

Theoretical formulation and adopted boundary procedure

This section briefly gives the governing problem and the relevant bondary-integral equations employed at each time step for one bubble interacting with one solid particle (case $M = N = 1$). For further details the reader is directed to where the theory is presented for the general case of a collection of $M \geq 1$ bubble(s) and $N \geq 1$ solid particle(s).

Axisymmetric governing Stokes flow problem

We consider a solid particle $\mathcal{P}$ and a bubble $\mathcal{B}$ immersed in a Newtonian liquid, with uniform viscosity μ and density ρ, migrating under the action of a uniform gravity field $\mathbf{g} = -g\mathbf{e}_3$ towards a

free surface. At time t the solid has boundary $\Sigma(t)$, the bubble has surface $S_1(t)$ with uniform surface tension γ_1 and the free surface with uniform surface tension γ_0 is denoted by $S_0(t)$. As sketched in Figure 1, all surfaces moreover admit the same axis of revolution $(0, \mathbf{e}_3)$.

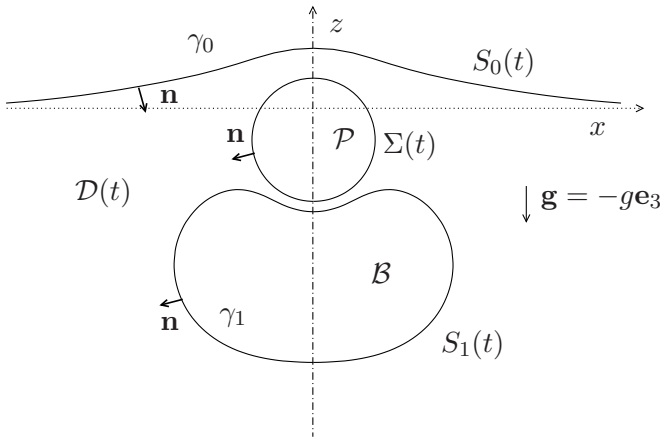

Figure 1: Two interacting bubble $\mathcal{B}$ and solid sphere $\mathcal{P}$ ascending near the free surface $S_0(t)$. At initial time $t = 0$ the bubble is spherical with radius a while the solid particle has radius $a/2$. The plotted shapes are the computed ones at normalized time $\overline{t} = 1.90$ for $\mathrm{Bo} = \rho g a^2/(3\gamma_1) = 2$ (see also Figure 2 (c) in the section devoted to the numerical results).

At initial time $t = 0$ the free surface is the $x_3 = 0$ plane with pressure p_0, the bubble is spherical with radius a and all surface are separated. At each time $t > 0$ the axisymmetric flow in the liquid domain $\mathcal{D}(t)$ has pressure $p+\rho\mathbf{g}.\mathbf{x}+p_0$ and velocity $\mathbf{u}$ with typical magnitude $V > 0$. The solid particle, with *uniform* density ρ_s and length scale $a_s \leq O(a)$, translates (no rotation for symmetry reasons) at the velocity $U(t)\mathbf{e}_3$ whereas the bubble has constant volume $\mathcal{V}$ and constant pressure p_1. Assuming that $\mathrm{Re} = \rho V a/\mu \ll 1$, the flow $(\mathbf{u}, p)$ with stress tensor $\boldsymbol{\sigma}$ then obeys the following quasi-steady Stokes flow problem

$$\boldsymbol{\nabla} \cdot \mathbf{u} = 0 \text{ and } \mu \boldsymbol{\nabla}^2 \mathbf{u} = \mathbf{grad} p \text{ in } \mathcal{D}(t), \ (\mathbf{u}, p) \to (\mathbf{0}, 0) \text{ as } |\mathbf{x}| \to \infty, \tag{1}$$

$$\boldsymbol{\sigma} \cdot \mathbf{n} = (\rho \mathbf{g} \cdot \mathbf{x} + \gamma_0 \boldsymbol{\nabla}_S \cdot \mathbf{n})\, \mathbf{n} \text{ on } S_0(t), \ \boldsymbol{\sigma} \cdot \mathbf{n} = (\rho \mathbf{g} \cdot \mathbf{x} - p_1 + \gamma_1 \boldsymbol{\nabla}_S \cdot \mathbf{n})\, \mathbf{n} \text{ on } S_1(t), \tag{2}$$

$$\mathbf{u} = U(t)\mathbf{e}_3 \text{ on } \Sigma(t) \tag{3}$$

where $\mathbf{n}$ denotes the unit normal on the liquid domain boundary directed into the liquid and $H = [\boldsymbol{\nabla}_S \cdot \mathbf{n}]/2$ designates the local average curvature. The solid particle with volume $\mathcal{V}_s$ has negligible inertia and therefore is to be force-free. Accordingly, one requires the additional condition

$$\int_{\Sigma(t)} \mathbf{e}_3 \cdot \boldsymbol{\sigma} \cdot \mathbf{n} dS = (\rho_s - \rho)\mathcal{V}_s\, g. \tag{4}$$

In a similar fashion, the bubble is also force-free. Such a property reads $\int_{S_1(t)} \mathbf{e}_3 \cdot \boldsymbol{\sigma} \cdot \mathbf{n} dS = -\rho \mathcal{V} g$. It is however already satisfied by integrating on the bubble surface $S_1(t)$ the boundary condition (2) there (since γ_1 is uniform). Finally, since the bubble has time-independent volume, (1)-(4) is also supplemented with the key relation

$$\int_{S_1(t)} \mathbf{u} \cdot \mathbf{n}\, dS = 0. \tag{5}$$

In summary, one has to solve for the unknown flow $(\mathbf{u}, p)$ *and* solid particle velocity $U(t)\mathbf{e}_3$ the equations and boundary conditions (1)-(3) in conjunction with the requirements (4)-(5).

Auxiliary Stokes flow and boundary method

As shown in [3], a trick actually permits one to determine the velocity $U(t)\mathbf{e}_3$ without solving the entire problem! It appeals to the auxiliary Stokes flow $(\mathbf{u}', p')$, with stress tensor $\boldsymbol{\sigma}'$, obeying (1) and the following boundary conditions and relation

$$\boldsymbol{\sigma}' \cdot \mathbf{n} = \mathbf{0} \text{ on } S_0(t) \cup S_1(t), \ \mathbf{u}' = \mathbf{e}_3 \text{ on } \Sigma(t), \int_{S_1(t)} \mathbf{u}' \cdot \mathbf{n} \, dS = 0. \tag{6}$$

As seen in [3], once the resulting traction $\boldsymbol{\sigma}' \cdot \mathbf{n}$ on $\Sigma(t)$ and velocity $\mathbf{u}'$ on the surface $S_0(t) \cup S_1(t)$ are gained, the velocity $U(t)$ is then obtained from the relation (easily deduced from the usual reciprocal identity [4])

$$\left[\int_{\Sigma(t)} \mathbf{e}_3 \cdot \boldsymbol{\sigma}' \cdot \mathbf{n} \, dS \right] U(t) = (\rho - \rho_s) \mathcal{V}_s \, g + \sum_{m=0}^{1} \int_{S_m(t)} \mathbf{u}' \cdot (\rho \mathbf{g} \cdot \mathbf{x} + \gamma_m \boldsymbol{\nabla}_S \cdot \mathbf{n}) \, \mathbf{n} \, dS. \tag{7}$$

Accordingly, it is sufficient to successively obtain the unknown velocity on $S_0(t) \cup S_1(t)$ and the surface traction on the solid particle boundary $\Sigma(t)$ for two similar problems consisting of (1)-(3) and (5): the first one for the auxiliary flow $(\mathbf{u}', p')$ and the second one (after calculating $U(t)$ from (5)) for the liquid flow $(\mathbf{u}, p)$. This is done by solving two coupled boundary-integral equations and the relation (5). More precisely as it is shown in [3], one has here to solve the

$$\begin{aligned} -8\mu\pi \mathbf{u}(\mathbf{x}) + \mu \int_{S_0(t) \cup S_1(t)} [\mathbf{u}(\mathbf{y}) - \mathbf{u}(\mathbf{x})] \cdot \mathbf{T}(\mathbf{y}, \mathbf{x}) \cdot \mathbf{n}(\mathbf{y}) dS - \int_{\Sigma(t)} \mathbf{G}(\mathbf{y}, \mathbf{x}) \cdot [\boldsymbol{\sigma} \cdot \mathbf{n}](\mathbf{y}) dS \\ = \int_{S_0(t) \cup S_1(t)} \mathbf{G}(\mathbf{y}, \mathbf{x}) \cdot [\boldsymbol{\sigma} \cdot \mathbf{n}](\mathbf{y}) dS \text{ for } \mathbf{x} \text{ on } S_0(t) \cup S_1(t), \end{aligned} \tag{8}$$

$$\begin{aligned} \mu \int_{S_0(t) \cup S_1(t)} \mathbf{u}(\mathbf{y}) \cdot \mathbf{T}(\mathbf{y}, \mathbf{x}) \cdot \mathbf{n}(\mathbf{y}) dS - \int_{\Sigma(t)} \mathbf{G}(\mathbf{y}, \mathbf{x}) \cdot [\boldsymbol{\sigma} \cdot \mathbf{n}](\mathbf{y}) dS \\ = 8\mu\pi \mathbf{u}(\mathbf{x}) + \int_{S_0(t) \cup S_1(t)} \mathbf{G}(\mathbf{y}, \mathbf{x}) \cdot [\boldsymbol{\sigma} \cdot \mathbf{n}](\mathbf{y}) dS \text{ for } \mathbf{x} \text{ on } \Sigma(t), \end{aligned} \tag{9}$$

$$\int_{S_1(t)} \mathbf{u} \cdot \mathbf{n} \, dS = 0 \tag{10}$$

where the second-rank velocity $\mathbf{G}$ and associated third-rank stress tensor $\mathbf{T}$ are defined in [4].

Implementation and preliminary numerical results

This section gives a few informations on the employed numerical strategy and also provides numerical results for a neutrally buoyant solid sphere interacting with one bubble and a free surface having identical surface tensions.

Implementation

Since the problem is axisymmetric, cylindrical coordinates (r, ϕ, z) with $r = \sqrt{x^2 + y^2}$, $z = x_3$ and ϕ the azimuthal angle in the range $[0, 2\pi]$ are employed. The traces $\mathcal{L}_m$ of Σ_m for $m = 0, 1$ and $\mathcal{L}$ of Σ in the $\phi = 0$ half plane are also introduced. Then, performing an integration of the boundary problem (8)-(10) over ϕ yields another boundary problem involving the previous contours $\mathcal{L}_0, \mathcal{L}_1$ and $\mathcal{L}$. This latter problem is solved by a boundary element technique after truncating the unbounded contour $\mathcal{L}_0$. As explained in [1], the numerical treatment of the resulting linear system appeals to a discrete Wielandt's deflation method.

In practice, we track in time the (truncated) free surface $S_0(t)$, the bubble surface $S_1(t)$ and the solid particle boundary $\Sigma(t)$ by running a Kutta-Fehlberg algorithm. At time t, the knowledge of those surfaces makes it possible to calculate the curvature there, then the solid sphere velocity $U(t)$ and finally the liquid velocity $\mathbf{u}$ on the liquid domain boundary. For a time step Δt the new surfaces at time $t + \Delta t$ are obtained by advancing the fluid boundary with the displacement vector $\Delta t(\mathbf{u}.\mathbf{n})\mathbf{n}$.

Numerical results for a neutrally-buoyant solid sphere

We further present numerical results for a solid sphere with uniform density ρ_s and radius a_s interacting with a bubble and a free surface of identical surface tensions $\gamma_1 = \gamma$. Morevover, as it appears in liquid glass, the sphere is neutrally buoyant with $\rho_s/\rho = 0.94$ (a value encountered in glass process). When distant from the sphere and the free surface the bubble $\mathcal{B}$ is spherical with radius a and migrates at the velocity $V\mathbf{e}_3$ (the one obtained in an unbounded liquid) given by $V = \rho g a^2/(3\mu)$. Note that because its volume is preserved as time evolves $\mathcal{B}$ has length scale a.

Henceforth, we take $2a$ and $2a/V$ as length and velocity scale, respectively. Therefore, the normalized time $\overline{t}$ is $\overline{t} = \rho g a t/(6\mu)$. Finally, the Bond number Bo which compares at the bubble surface the "gravity" term $\rho\mathbf{g}.\mathbf{x}$ with the capillary "term" $\gamma_1 \boldsymbol{\nabla}_S \cdot \mathbf{n}$ is here defined as $\mathrm{Bo} = \rho g a^2/(3\gamma_1)$.

Let us first take $a_s = a/2$ and $\mathrm{Bo} = 2$ and put at initial time $\overline{t} = 0$ the solid sphere between the spherical bubble and the undisturbed free surface, the initial gaps between the sphere and each other surface being equal to a.

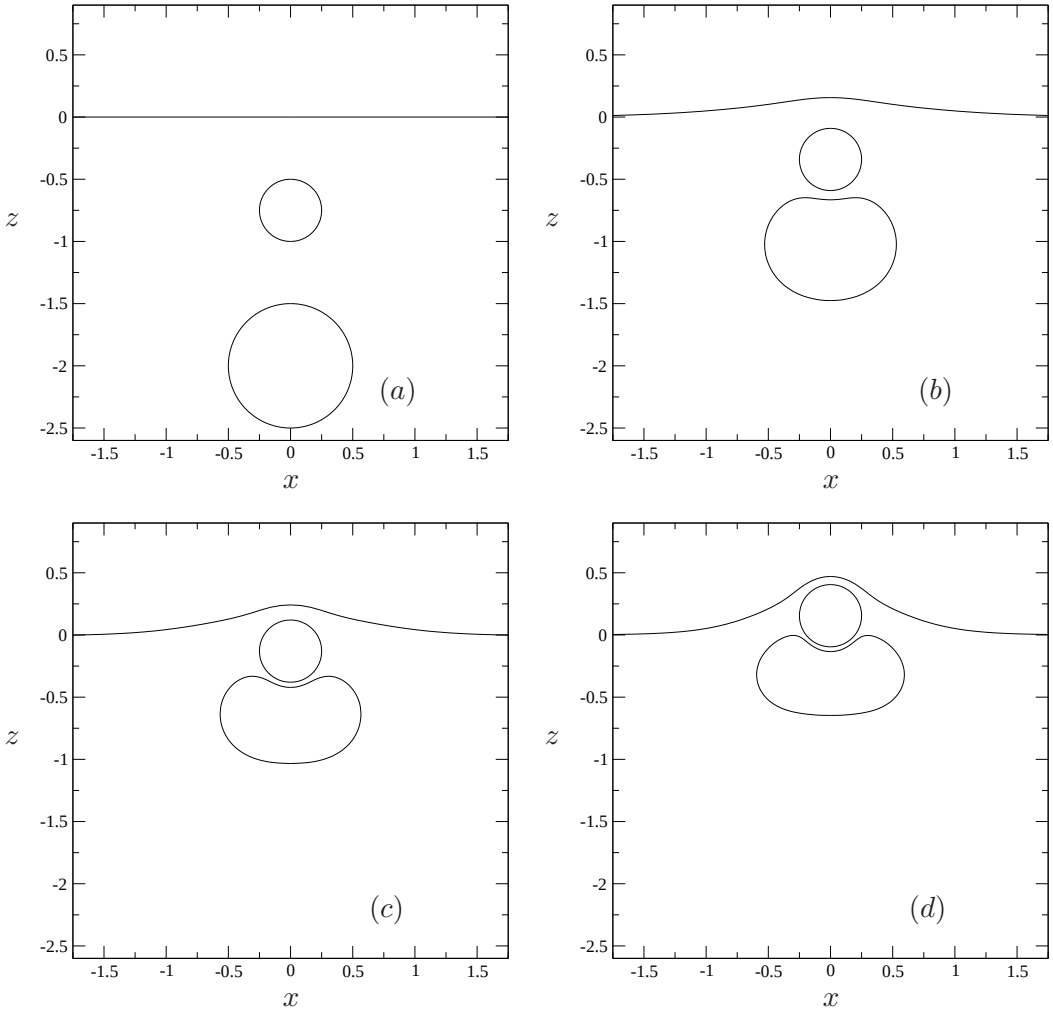

Figure 2: Computed free surface, bubble and solid sphere locations and shapes for $\mathrm{Bo} = 2$ at different normalized times: $\overline{t} = 0$ (a), $\overline{t} = 0.120$ (b), $\overline{t} = 1.90$ (c) and $\overline{t} = 2.72$ (d).

As seen in Figure 2, two different regimes are found as time evolves. In a first "fast" regime the bubble ascends faster than the solid sphere and the sphere-bubble gap therefore decreases faster than the gap between the sphere and the free surface whereas the free surface is weakly deformed (compare Figure 2(a) with Figure 2(b)). In a second "slow" regime, illustrated in Figure 2(c) and Figure 2(d), the bubble and the sphere slowly migrate towards the free surface which now experiences a slight deformation due to the combined action of the sphere and the bubble. In this regime liquid films take place below and above the solid sphere with the film below being the thinner one.

Not surprisingly, the computed shapes also depend upon the free-surface and bubble surface tensions $\gamma_1 = \gamma_0$. This is illustrated by plotting in Figure 3 the obtained shapes for Bo $= 1, 2$ at different normalized times $\overline{t}$ starting with the same initial configuration.

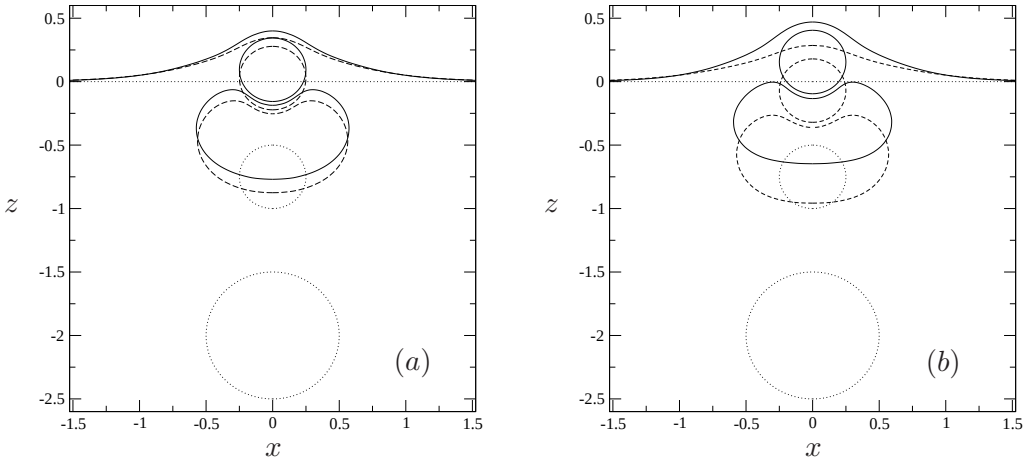

Figure 3: Compared shapes obtained at three different normalized times $\overline{t}_0 = 0, \overline{t}_1 = 1.19$ and $\overline{t}_2$ for $a_s = a/2$ at two different Bond numbers. (a) Bo $= 1$ and $\overline{t}_2 = 2.58$. (b) Bo $= 2$ and $\overline{t}_2 = 2.72$.

When the surface tension is weaker (case of Bo $= 1$ depicted in Figure 3(a)) the bubble is less "flexible" and thus speeds up more the solid sphere (compared the sphere locations at time $\overline{t} = 1.20$ in Figure 3(a) and Figure 3 (b)) during the previously-distinguished "fast" regime. In addition, for this ratio $a_s = a/2$ the deformation of the free surface at $\overline{t} = 1.20$ appears to be larger for Bo $= 1$ than for Bo $= 2$ although the surface tension there is larger. Not surprisingly, during the second "slow" regime in which the drainage of both thin films really takes place the free surface deformation for Bo $= 2$ finally is more pronounced than for Bo $= 1$.

In absence of sphere one would obtain (see [1]) a larger deformation of the free surface at each normalized time $\overline{t}$ for Bo $= 2$. This actually also occurs when the sphere is sufficiently small compared to the bubble. We illustrate this behaviour in Figure 4 for the case for $a_s = a/4$.

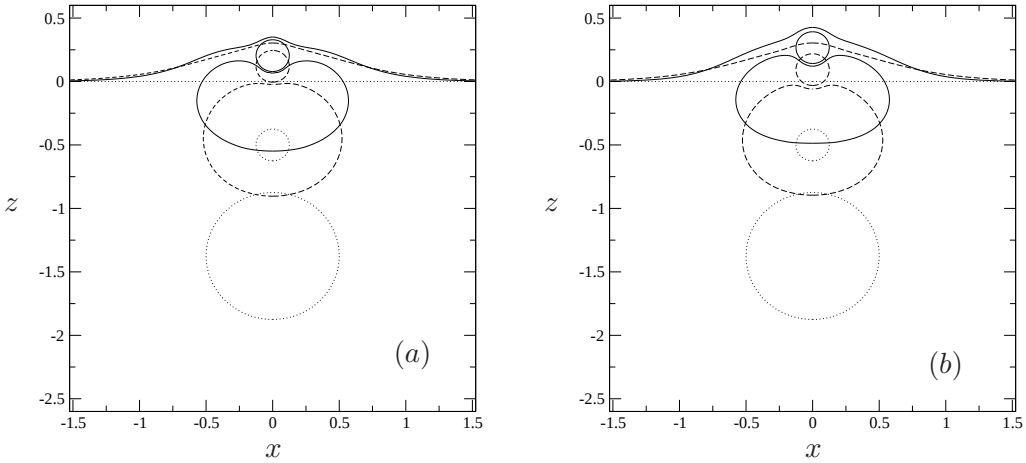

Figure 4: Compared shapes obtained at three different normalized times $\overline{t} = 0, \overline{t} = 1.19$ and $\overline{t} = 2.03$ for $a_s = a/4$ at two different Bond numbers. (a) Bo $= 1$. (b) Bo $= 2$.

Conclusions

Our preliminary results for a nearly neutrally buoyant sphere reveal that the obtained final configuration (free surface shape) is strongly sensitive to the sphere size (compared to the bubble) and

to the Bond number. Additional results will be given and discussed at the oral presentation with attention also paid to the case of inequal free surface and bubble surface tensions γ_0 and γ_1.

References

[1] F. Pigeonneau and A. Sellier. Low-Reynolds-Number gravity-driven migration and deformation of bubbles near a free surface. *Phys. Fluids*, 23:092102, 2011.

[2] M. Guémas, F. Pigeonneau, and A. Sellier. Gravity-driven migration of one bubble near a free surface: surface tension effects. In P. Prochazca and M. H. Aliabadi, editors, *Advances in Boundary Element & Meshless Techniques XIII*, pages 115–120. EC Ltd, UK, 2012.

[3] M. Guémas, F. Pigeonneau, and A. Sellier. Gravity-driven migration of bubbles and/or solid particles near a free surface. In A. Sellier and M. H. Aliabadi, editors, *Advances in Boundary Element & Meshless Techniques XIV*, pages 400–405. EC Ltd, UK, 2013.

[4] S. Kim and S. J. Karrila. *Microhydrodynamics. Principles and selected applications.* Martinus Nijhoff Publishers, The Hague, 1983.